Long-term Photo-degradation of Nanofibrous Composites Based on Poly(3-hydroxybutyrate) Electrospun Fibers Loaded with Zinc Oxide Nanoparticles

Heriberto Rodríguez-Tobías, Graciela Morales, Hortensia Maldonado-Textle, Daniel Grande

Long-term photo-degradation of nanofibrous composites based on poly(3-hydroxybutyrate) electrospun fibers loaded with zinc oxide nanoparticles

Heriberto Rodríguez-Tobías [a], Graciela Morales [a], Hortensia Maldonado-Textle [a], Daniel Grande [b*]*

[a] *Centro de Investigación en Química Aplicada, Blvd. Enrique Reyna No. 140, C.P. 25294, Saltillo, Coahuila, Mexico.*

[b] *Univ Paris Est Creteil, CNRS, Institut de Chimie et des Matériaux Paris-Est (ICMPE), UMR 7182, 2 rue Henri Dunant, 94320 Thiais, France.*

Submitted as a regular article to *Fibers and Polymers*

* Corresponding authors:

Heriberto Rodríguez Tobías

Phone: + 52 (844) 4 38 98 30

E-mail: lcq.heriberto.rodriguez@gmail.com

Dr. Graciela Morales

Phone: + 52 (844) 4 38 98 30

E-mail: graciela.morales@ciqa.edu.mx

Dr. Daniel Grande

Phone: +33 (0)1 48 7 12 10

E-mail: daniel.grande@cnrs.fr

ABSTRACT

Composite mats based on submicron biopolyester fibers and zinc oxide (ZnO) nanoparticles have been exploited in medicine and environmental areas, as antibacterial wound dressings or filters. Generally, the resulting mats have to be subjected to UV irradiation in order to promote the formation of reactive oxygen species, thus activating the antimicrobial or photocatalytic effect of ZnO. Therefore, investigation related to the influence of ZnO on poly(3-hydroxyalkanoate) photo-degradation is required. In this context, the present paper addresses the long-term photo-degradation of nanofibrous poly(3-hydroxybutyrate) (PHB)/ZnO composites derived from two complementary electro-hydrodynamic techniques, namely electrospinning or electrospinning/electrospraying tandem processes.

A thorough investigation of the as-obtained PHB/ZnO fibrous composites implying the utilization of ATR-FTIR, SEC, and SEM was performed before and after artificial UV aging for a period of time of 500 h in order to evaluate the effect of the electro-hydrodynamic technique and ZnO content on the UV shielding properties of composite mats.

Keywords

Photo-degradation; electrospinning; electrospraying; poly(3-hydroxybutyrate); zinc oxide nanoparticles

1. INTRODUCTION

Electrospinning-based techniques have demonstrated to be practical and economically viable processes for manufacturing polymeric fibers in the submicron scale with controlled morphological features, such as average fiber diameter, porosity ratio, fiber orientation, and in the case of composite fibers, nanoparticles distribution (on fiber surface or embedded within fibers) [1-3]. In this regard, the control of the aforementioned features of fibrous polymer materials make them ideal candidates for the design and fabrication of prototypes with high potential to solve environmental and health concerns, including filters for the elimination of a wide range of chemical and biological contaminants in air or water, and antimicrobial and/or wound healing mats [1, 4-9]. It is noteworthy that (bio)polyesters, such as polylactides and poly(3-hydroxyalkanoate)s (PHAs) have been extensively used for developing the aforementioned prototypes, mainly due to their renewability, biocompatibility and/or biodegradability [6-12].

Furthermore, the incorporation of metal oxide nanoparticles into (bio)polyester-based fibers can be considered as a synergistic approach to develop devices with improved antimicrobial and photocatalytic properties. In this regard, zinc oxide (ZnO) nanoparticles are well-known antimicrobial and photocatalytic nanostructures which can be used as multi-functional nanomaterials able to eliminate several chemical pollutants and microorganisms without collateral risks for human health and/or other species, since ZnO is catalogued as a safe component by the Food and Drug Administration [13-20].

It is needed to emphasize that there is a scarcity of publications related to PHA/ZnO electrospun composites, and the majority of them are focused on the fabrication of mats and complemented with some relevant characterization associated with the structure and morphology of the resulting fibers. As an example, Yu *et al*. [21] electrospun a mixed solution of poly(3-hydroxybutyrate-*co*-3-hydroxyvalerate) (PHBHV)/ZnO, whereby composite fibers with 300 nm in size were thus obtained. The authors argued that the formation of hydrogen bonding favored the dispersion of ZnO nanoparticles into the PHBHV fibers, and they also demonstrated that the nanometal oxide restricted the crystallization. Moreover, Naphade *et al.* [22] obtained PHBHV/ZnO electrospun fibers ranging from 700 to 800 nm with enhanced UV emission properties which could lead to the development of biomarkers. Zviagin *et al*. [23] also reported the generation of poly(3-hydroxybutyrate) (PHB) fibers by electrospinning in combination with hydrothermal deposition of ZnO nanostructures, and the mats thus obtained were used for the design of piezoelectric devices.

A handful number of researchers has studied the generation of antimicrobial PHA/ZnO fibrous devices derived from electrospinning techniques. Lagaron's research group proved the antimicrobial activity of electrospun PHBHV/ZnO mats against *Escherichia coli*, *Staphylococcus aureus,* and *Listeria monocytogenes*. They also analyzed the effect of ZnO content on morphological, mechanical, thermal, and optical properties of the resulting electrospun materials [24, 25]. Our research consortium has also exploited the electrospinning process and its combination with the electrospraying technique for designing antimicrobial PHB/ZnO mats, whose thermal and mechanical performance was evaluated [19].

As it can be noticed in the aforementioned publications, many efforts have been made to design PHBHV or PHB mats containing ZnO nanoparticles as antimicrobial agents. However, there is no investigation related to the photo-degradation of resulting fibrous materials, which is of outmost interest due to the activation or increase of antimicrobial and/or photocatalytic activity promoted by UV irradiation, which in turn could lead to photo-degradation and, eventually, a reduction of the fibrous materials lifetime.

In this context, the aim of the present work is to investigate the photo-degradation behavior of two types of PHB-based fibrous composites, namely ZnO-embedded PHB submicron fibers engineered by mere electrospinning of the corresponding solution/dispersion, and ZnO-coated PHB submicron fibers derived from the electrospinning/electrospraying tandem technique. Further spectroscopic, chromatographic, and microscopic analyses were performed to evaluate the effect of the aging time, the employed electrohydrodynamic technique, and ZnO nanoparticles concentration/dispersion on structural and morphological changes of the PHB-based fibrous composites.

2. EXPERIMENTAL

2.1. Materials

Commercially available poly(3-hydroxybutyrate) (PHB) (Biomer, $\bar{M}_n$= 144,000 g·mol^{-1}, $\bar{M}_w/\bar{M}_n$= 2.3) and 2,2,2-trifluoroethanol (TFE) from Sigma-Aldrich were used as solute and solvent, respectively, of precursory solutions which eventually were subjected to the electrospinning-based techniques for generation of the fibrous materials. ZnO

nanoparticles (12 nm in diameter and distribution ranging from 8 to 20 nm) were obtained by microwave-assisted synthesis as previously reported [26-28].

2.2. Fabrication of fibrous materials

Fibrous PHB composites were engineered by two electrospinning-based technologies:

(a) mere electrospinning of PHB solutions (10 wt-% in TFE) containing 1-5 wt-% of ZnO nanoparticles relative to polymer, at a flow rate of 2.7 $mL \cdot min^{-1}$, voltage of 25 kV, cylindrical collector speed of 700 rpm, and a needle-to-collector distance of 25 cm

(b) tandem process based on the electrospinning of a PHB solution (10 wt-% in TFE) and the simultaneous electrospraying of a ZnO nanoparticles dispersion in MeOH (1-5 wt-% respect to PHB and dispersed by ultrasound bath for 1.5 h). The electrospinning was conducted under the same conditions as those used in (a), while electrospraying was carried out with a collector-to-needle distance of 5 cm and the syringe being placed at an angle of 120° relative to the direction of the other syringe.

2.3. Artificial UV aging of PHB fibers and PHB/ZnO fibrous composites

Aging of fibrous PHB composites (2 × 2 cm samples) was conducted in a UV accelerated weathering tester (Q-Lab) equipped with a lamp at fixed wavelength and irradiance, *i.e.* 313 nm and 0.87 W·m2, respectively, and temperature of 60°C. Several samples were withdrawn at different aging times (50, 100, 250, and 500 h) for characterizing them by different

physico-chemical techniques described in subsequent sections. It should be stressed that the wavelength was comprised within the range commonly used for activating metal oxide photocatalytic properties (UVA and UVB regions), which could be beneficial to promote antibacterial activity [13-20].

2.4. Characterization of fibrous materials

A scanning electron microscope (SEM, JEOL JSM-7401F) coupled with an energy dispersive X-ray (EDX) detector was used to analyze the morphology and composition of the as-obtained and aged mats. In addition, inner morphology of the obtained PHB mats was analyzed by a FEI Titan 80-200 transmission electron microscope (TEM). Average fiber diameter was estimated by using *ImageJ* software. For this purpose, several SEM micrographs were analyzed, and the diameter was estimated from 4-5 sections along 60-70 fibers (*ca*. 250-300 counts).

Mercury intrusion porosimetry (MIP) analyses were performed with a Micrometrics Autopore IV equipment. The porosity features were determined by using the Washburn equation between the applied pressure (from 1.03 to 206.8 MPa) and the pore diameter into which mercury intruded, thus obtaining defined values for porosity ratio and pore size distribution from which the average pore size was estimated.

To identify any chemical change of the aged PHB/ZnO mats, infrared spectra were recorded on a Nicolet Nexus spectrometer in the attenuated total reflection mode (ATR-FTIR) between 4000 and 600 cm^{-1}, with 32 scan summations and a 4 cm^{-1} resolution.

Molar masses of aged fibrous PHB composites were estimated by size-exclusion chromatography (SEC), using three PL-gel columns with a refraction index detector at 40°C and THF (HPLC grade) as the eluent at a flow rate of 1 $mL \cdot min^{-1}$. Polystyrene standards were employed for calibration.

3. RESULTS AND DISCUSSION

3.1. Morphologic features of PHB/ZnO fibrous composites before UV irradiation

Morphology of fibrous materials derived from electrospinning techniques is of paramount significance since their applicability as filter media depends on several morphological characteristics, namely average fiber diameter ($\overline{D}_f$), porosity ratio (P), and average pore size ($\overline{D}_p$). In this context, fibrous materials based on PHB and ZnO nanoparticles were analyzed by means of SEM and MIP (**Table 1**).

<Table 1>

The results gathered in **Table 1** demonstrated that the concentration of ZnO nanoparticles in the precursory solution or their deposition on the fiber surface by electrospraying had a negligible influence on the morphological features of PHB-based mats, since all materials exhibited $\overline{D}_f$ values from 400 to 600 nm approximatively, P values ranging from 83 to 90 %, and $\overline{D}_p$ values from 1.1 to 2.2 µm. Our research consortium evidenced that the similarity of the morphological features associated with mats derived from mere electrospinning was due to the fact that the electrical conductivity and viscosity of the precursory PHB solutions remained practically unchanged by the presence of ZnO

nanoparticles [19]. In the case of the PHB mats derived from the electrospinning/electrospraying technique, the process was performed by using neat PHB precursory solutions, therefore, the ZnO nanoparticles sprayed on the fibers did not affect the aforementioned morphological features [19].

ZnO nanoparticles dispersion in/on the PHB fibers was assessed by means of electron microscopic techniques. In this regard, **Figure 1** shows some TEM and SEM micrographs of the obtained materials, in which a homogeneous dispersion of ZnO was achieved in electrospun PHB fibers (**Figure 1a,b**), while electrospun/electroprayed PHB fibers exhibited some ZnO aggregates with sizes ranging from 300 to 4000 nm (**Figure 1c-f**). Some of these aggregates were semi-exposed on the fiber surface. These analyses evidenced that the electrospraying technique, under the experimental conditions herein used, was not suitable for obtaining well-dispersed ZnO nanoparticles, which could affect the final photo-degradation behavior of PHB/ZnO composite fibers. This issue will be addressed in subsequent sections.

<Figure 1>

3.2. Structures of electrospun PHB/ZnO mats after UV irradiation

Metal oxide nanoparticles, such as TiO_2 or ZnO, exhibit photocatalytic activity when subjected to UV irradiation. Therefore, the presence of these nanoparticles within electrospun polyester fibers could trigger their photo-degradation. In this context, Sadi *et al.* [29] have extensively studied the photo-degradation of PHB in bulk, concluding that the degradation of PHB chains leads to a chemi-crystallization process, which can be evidenced by FTIR changes of carbonyl and C-O-C signals.

In this regard, **Figure 2** shows FTIR spectra of neat and UV-irradiated electrospun PHB mats. In general, neat PHB mats displayed a signal centered at 1722 cm^{-1} which corresponded to carbonyl (C=O) stretching of the crystalline phase, along with a shoulder at higher wavenumber (1745 cm^{-1}) associated with C=O stretching of the amorphous phase. In the crystalline phase, the C=O groups were close to the hydrogen atoms of a vicinal PHB chain, which reduced the polar momentum, thus provoking C=O vibrations at lower wavenumber (1722 cm^{-1}). Additionally, two signals corresponding to stretching vibrations of C-O-C bonds were present at 1186 and 1230 cm^{-1}, the first one related to the amorphous phase and the second one associated to the crystalline phase [29, 30].

<Figure 2>

Since the photo-degradation of PHB promotes chemi-crystallization of the resulting polymeric chains, the monitoring of the aforementioned FTIR signals can provide information about the effect of UV irradiation time, ZnO concentration and electro-hydrodynamic technique on the PHB-based composite mats. However, carbonyl signals were overlapped, therefore only the C-O-C were considered for this monitoring. **Figure 3** displays the absorbance at 1230 cm^{-1} to absorbance at 1186 cm^{-1} ratio (A_{1230}/A_{1186}) as a function of irradiation time and ZnO content. In general, all materials exhibited a substantial increase of A_{1230}/A_{1186} ratio at 50 h of irradiation time, followed by a slight increase at 250 h, and finally this ratio exhibited a plateau at 500 h, thus suggesting the increase in the crystallinity of polymer chains.

Figure 3 could also be considered to investigate the effect of ZnO concentration and the implemented electrospinning technique. In the case of the electrospun PHB mats, the

presence of low ZnO concentration (1 and 3 wt-%) did not change the pattern of the A_{1230}/A_{1186} ratio as a function of irradiation time, which could be interpreted as these mats exhibited similar levels of crystalline phase formation associated with photo-degradation. A significant reduction of A_{1230}/A_{1186} ratio was observed only at the highest ZnO concentration (*i.e.*, 5 wt-%), which could be attributed to the UV protection by the semi-exposed ZnO nanoparticles/aggregates as displayed by SEM/TEM analyses. On the other hand, the electrospun/electrosprayed PHB mats exhibited a quite different performance, since the UV protection was the highest when the fibers contained the lowest ZnO concentration (1 wt-%). At higher ZnO concentrations (3 and 5 wt-%), a shielding effect against photo-degradation was not perceived. This behavior could be explained in terms of ZnO nanoparticles aggregation when ZnO concentration was equal to or higher than 3 wt-%, as shown by elemental mapping (see **Figure 1e,f**), thus reducing the ZnO surface prone to absorb the UV irradiation [10, 31-33].

<Figure 3>

To further analyze the photo-degradation of electrospun PHB/ZnO composite fibers, the evolution of number-average molar mass (M_n) associated with PHB as a function of both UV irradiation time and ZnO content is plotted in **Figure 4a**. Firstly, a reduction of M_n values was noticed (decreasing from 144 to 25-35 $kg \cdot mol^{-1}$) as UV irradiation times increased and the major molar mass loss occurred at the early stage (50 h). On the other hand, a slight UV-shielding effect was perceived at the highest ZnO content, which could be evidenced by a higher M_n value, thus corroborating the UV absorption by the exposed nanoparticles/aggregates. Moreover, the photo-degradation of PHB/ZnO mats induced a widening of the molar mass distributions (M_w/M_n) as demonstrated in **Figure 4b**. Generally,

M_w/M_n values increased with UV irradiation time, and no particular trend was noticed as a function of ZnO nanoparticles content.

<Figure 4>

Regarding the photo-degradation behavior of electrospun/electrosprayed PHB/ZnO fibrous materials, SEC analyses evidenced that the ZnO content and the tandem technique did not confer a shielding effect, since M_n values were lower than those of the fibers derived from mere electrospinning in all the range of UV irradiation time analyzed (see **Figure 5a**). M_n values were equal to 33-38 and 15-30 $kg \cdot mol^{-1}$ for 50 h and 250 h of UV irradiation time, respectively, and the evolution of the M_w/M_n values was practically similar to that exhibited by electrospun PHB/ZnO mats (see **Figure 5b**). These SEC results were in good agreement with those from the structural FTIR analyses previously discussed, *i.e.*, electrospun mats containing high ZnO content possessed a better resistance to UV, while the tandem electrospinning/electrospraying technique was not suitable to exert a significant shielding effect.

<Figure 5>

3.3. Morphologies of PHB/ZnO mats after UV irradiation

Electrospun fibrous devices for water decontamination or wound protection/healing may constitute efficient filters against pollutants and/or pathogenic microorganisms, as their high surface area-to-volume ratio favors the contact/interaction with the latters [26]. In this regard, the investigation of the effect of UV irradiation on the fibrous morphology of electrospun engineered materials is of outmost interest. In this context, **Figure 6** depicts the morphology of the PHB mats derived from the electrospinning of the corresponding solution

containing different ZnO concentrations (0, 1, 3, and 5 wt-%) depending on the UV irradiation time (0, 50, 250, and 500 h). All specimens showed a common morphological pattern, *i.e.*, PHB fibers were transformed into submicron rods, which can be explained by the combination of PHB chains scission and chemi-crystallization, eventually, forming submicron rods by fragmentation. This phenomenon was more pronounced when the irradiation time was longer, since it could be observed a significant reduction of the PHB rod size (from 5-10 μm to 1-2 μm). On the contrary, no particular effect of ZnO concentration could be perceived, since all PHB mats resulted in highly degraded rods.

Regarding the fibrous materials engineered by electrospinning of a PHB solution and electrospraying of ZnO dispersions (*i.e.*, 1-5 wt-%), the characteristic morphology gave evidence of a similar transformation than electrospun PHB mats under UV exposition during different periods of time. As a matter of evidence, **Figure 7** displays the corresponding SEM micrographs, in which it could be detected the previously explained morphology transformation pattern, *i.e.* electrospun/electrosprayed materials evolved from continuous fibers to discontinuous rods by chains scission and chemi-crystallization.

<Figure 6>

<Figure 7>

4. CONCLUSIONS

An extensive investigation of the photo-degradation behavior of ZnO-embedded and ZnO-coated PHB mats respectively engineered by electrospinning and

electrospinning/electrospraying techniques was undergone for the first time. In general, nano-ZnO within or deposited on the PHB fibers promoted a UV-shielding effect; nevertheless, FTIR and SEC analysis suggested a slightly higher extent of UV protection for the mats derived from mere electrospinning, which could be attributed to a better dispersion of ZnO nanoparticles on the PHB fiber surface. FTIR spectroscopy evidenced that UV irradiation promoted a chemi-crystallization of PHB chains whose occurrence was increased by extending the aging time. Further structural studies were performed by SEC analysis and electron microscopy (SEM and TEM) by which it was demonstrated that the exposition to UV rays led to substantial changes in the morphology and molecular changes, since the PHB/ZnO mats evolved from fibers to sub-micrometric rods with a reduction of molar mass regardless of the electro-hydrodynamic technique or ZnO content used.

Ultimately, it could be concluded that such fibrous PHB/ZnO composite mats have a high potential as wound dressings materials with good resistance to UV irradiation sterilization or membranes for UV-activated filters with a relatively short shelf life (~50 h).

ACKNOWLEDGMENTS

Financial support through French Mexican PCP program is gratefully acknowledged. The authors thank CONACyT (Mexico) for providing H. Rodríguez-Tobías with a Ph.D. grant. They also thank R. Pirès (CNRS, France) for his technical assistance in issues related to electron microscopy characterization.

CONFLICT OF INTEREST

All co-authors declare that there is no conflict of interest.

REFERENCES

1. M. Abrigo, S. L. McArthur, and P. Kingshott, *Macromol Biosci*, **14**, 772 (2014).
2. S. Agarwal, J. H. Wendorff, and A. Greiner, *Adv Mater*, **21**, 3343 (2009).
3. H. Rodríguez-Tobías, G. Morales, and D. Grande, *Mater. Sci. Eng. C*, **101**, 306 (2019).
4. R. Augustine, N. Kalarikkal, and S. Thomas, *Appl. Nanosci.*, **6**, 337 (2015).
5. P. Zahedi, I. Rezaeian, S.-O. Ranaei-Siadat, S.-H. Jafari, and P. Supaphol, *Polym. Adv. Technol.*, **21**, 77 (2010).
6. L. J. R. Foster, S. M. Davies, and B. J. Tighe, *J. Biomat. Sci. Polym. Ed.*, **12**, 317 (2012).
7. S. Philip, T. Keshavarz, and I. Roy, *J. Chem. Technol. Biotechnol.*, **82**, 233 (2007).
8. E. Renard, P.-Y. Tanguy, E. Samain, and P. Guerin, *Macromol. Symp.*, **197**, 11 (2003).
9. S. I. Yun, G. E. Gadd, B. A. Latella, V. Lo, R. A. Russell, and P. J. Holden, *Polym. Bull.*, **61**, 267 (2008).
10. K. Elena, S. Olya, M. Nevena, and R. Iliya, *Macromol. Biosci.*, **13**, 707 (2013).
11. J. Ramier, T. Bouderlique, O. Stoilova, N. Manolova, I. Rashkov, V. Langlois, E. Renard, P. Albanese, and D. Grande, *Mater. Sci. Eng. C Mater. Biol. Appl.*, **38**, 161 (2014).

12. K. Sombatmankhong, O. Suwantong, S. Waleetorncheepsawat, and P. Supaphol, *J. Polym. Sci. B Polym. Phys.*, **44**, 2923 (2006).

13. Y. W. Baek and Y. J. An, *Sci. Total. Environ.*, **409**, 1603 (2011).

14. R. Dastjerdi and M. Montazer, *Colloids Surf B Biointerfaces*, **79**, 5 (2010).

15. P. J. P. Espitia, N. d. F. F. Soares, J. S. d. R. Coimbra, N. J. de Andrade, R. S. Cruz, and E. A. A. Medeiros, *Food Bioprocess Technol.*, **5**, 1447 (2012).

16. M. Mirhosseini and F. B. Firouzabadi, *Int. J. Dairy Technol.*, **66**, 291 (2013).

17. G. Prado-Prone, P. Silva-Bermudez, A. Almaguer-Flores, J. A. Garcia-Macedo, V. I. Garcia, S. E. Rodil, C. Ibarra, and C. Velasquillo, *Nanomedicine*, **14**, 1695 (2018).

18. H. Rodríguez-Tobías, G. Morales, A. Ledezma, J. Romero, and D. Grande, *J. Mater. Sci.*, **49**, 8373 (2014).

19. H. Rodríguez-Tobías, G. Morales, A. Ledezma, J. Romero, R. Saldívar, V. Langlois, E. Renard, and D. Grande, *J. Mater. Sci.*, **51**, 8593 (2016).

20. R. Wahab, A. Mishra, S. I. Yun, Y. S. Kim, and H. S. Shin, *Appl. Microbiol. Biotechnol.*, **87**, 1917 (2010).

21. W. Yu, C.-H. Lan, S.-J. Wang, P.-F. Fang, and Y.-M. Sun, *Polymer*, **51**, 2403 (2010).

22. R. Naphade and J. Jog, *Fiber. Polym.*, **13**, 692 (2012).

23. A. S. Zviagin, R. V. Chernozem, M. A. Surmeneva, M. Pyeon, M. Frank, T. Ludwig, P. Tutacz, Y. F. Ivanov, S. Mathur, and R. A. Surmenev, *Eur. Polym. J.*, **117**, 272 (2019).

24. K. A.-O. Figueroa-Lopez, S. A.-O. Torres-Giner, D. Enescu, L. A.-O. Cabedo, M. A.-O. Cerqueira, L. M. Pastrana, and J. A.-O. X. Lagaron, *Nanomater.*, **10**, 506 (2020)

25. J. L. Castro-Mayorga, M. J. Fabra, A. M. Pourrahimi, R. T. Olsson, and J. M. Lagaron, *Food Bioprod. Process.*, **101**, 32 (2017).

26. A. Castro-Ruíz, H. Rodríguez-Tobías, G. A. Abraham, G. Rivero, and G. Morales, *J. Appl. Polym. Sci.*, **137**, 48429 (2020).

27. H. Rodríguez-Tobías, G. Morales, F. J. Enríquez-Medrano, and D. Grande, *Macromolecular Symposia*, **374**, 1600102 (2017).

28. H. Rodríguez-Tobías, G. Morales, A. Olivas, and D. Grande, *Macromol. Chem. Phys.*, **216**, 1629 (2015).

29. R. K. Sadi, G. J. M. Fechine, and N. R. Demarquette, *Polym. Degrad. Stab.*, **95**, 2318 (2010).

30. H. Ariffin, H. Nishida, Y. Shirai, and M. A. Hassan, *Polym. Degrad. Stab.*, **93**, 1433 (2008).

31. H. Rodríguez-Tobías, G. Morales, H. Maldonado-Textle, and D. Grande, *Polym. Degrad. Stab.*, **152**, 95 (2018).

32. Y. Zhu, G. G. Buonocore, M. Lavorgna, and L. Ambrosio, *Polym. Comp.*, **32**, 519 (2011).

33. A. M. Diez-Pascual and A. L. Diez-Vicente, *Int. J. Mol. Sci.*, **15**, 10950 (2014).

Table 1. Morphological features of electrospun and electrospun/electrosprayed PHB/ZnO fibrous mats.

ZnO content (wt-%)	$\overline{D}_f$ [a] (nm)		P [b] (%)		$\overline{D}_p$ [c] (µm)	
	E [d]	E/ES [e]	E	E/ES	E	E/ES
0	425 ± 170	425 ± 170	85	85	1.98 ± 1.40	1.98 ± 1.20
1	380 ± 140	475 ± 160	83	90	1.69 ± 1.20	1.54 ± 1.10
3	480 ± 190	600 ± 220	86	88	1.11 ± 0.70	1.46 ± 1.05
5	440 ± 210	669 ± 230	87	88	2.24 ± 1.50	1.79 ± 1.30

[a] Average fiber diameter as determined from SEM images by using the *ImageJ* software, the number after the ± symbol is the standard deviation. [b] Porosity ratio and [c] average pore size as determined by MIP, the number after the ± symbol is the standard deviation. [d] PHB/ZnO mats derived from mere electrospinning (E) and [e] obtained by combination of electrospinning/electrospraying (E/ES).

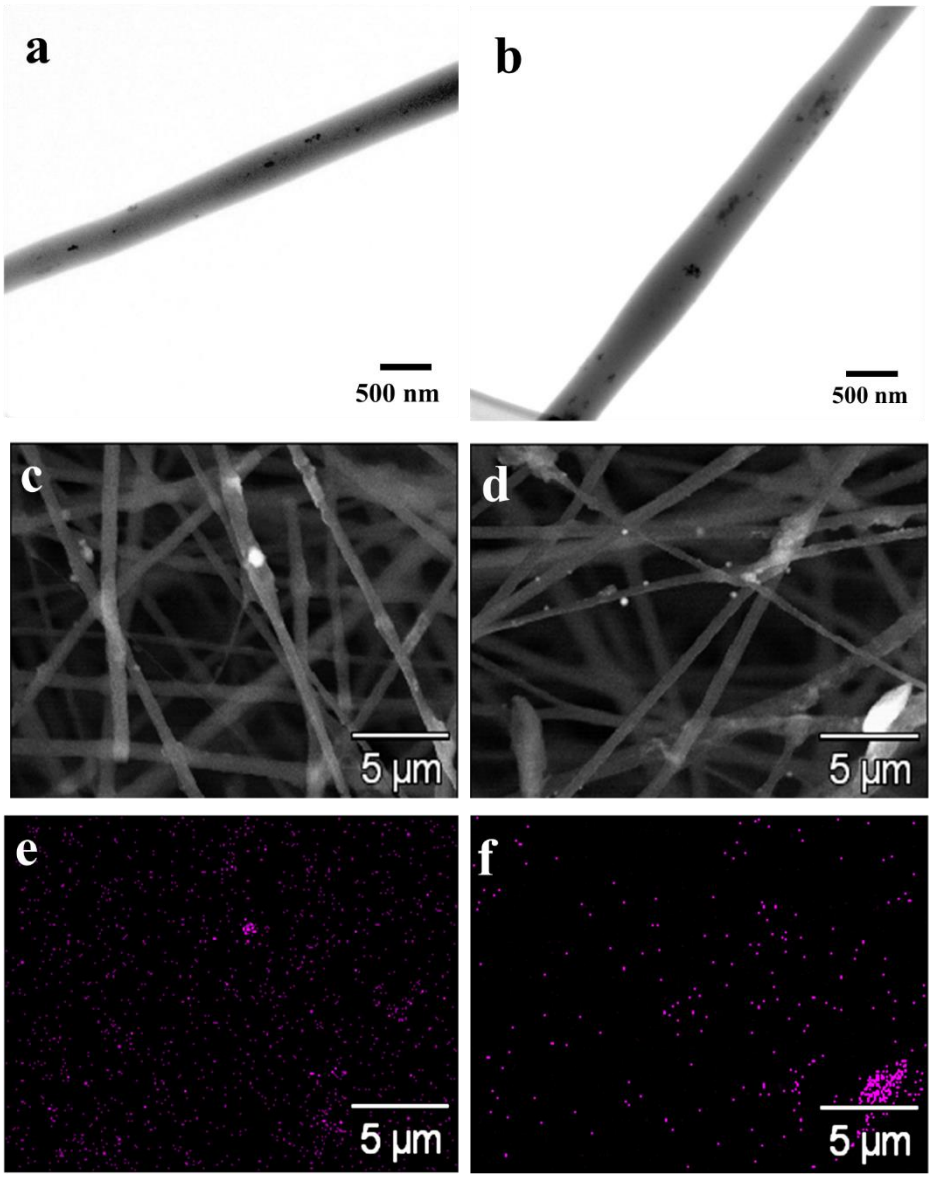

Figure 1. TEM images of (a,b) electrospun and SEM images of (c,d) electrospun/electrosprayed PHB fibers containing (a,c) 3 and (b,d) 5 wt-% ZnO nanoparticles. Elemental mapping of electrospun/electrosprayed PHB fibers containing (e) 3 and (f) 5 wt-% ZnO nanoparticles.

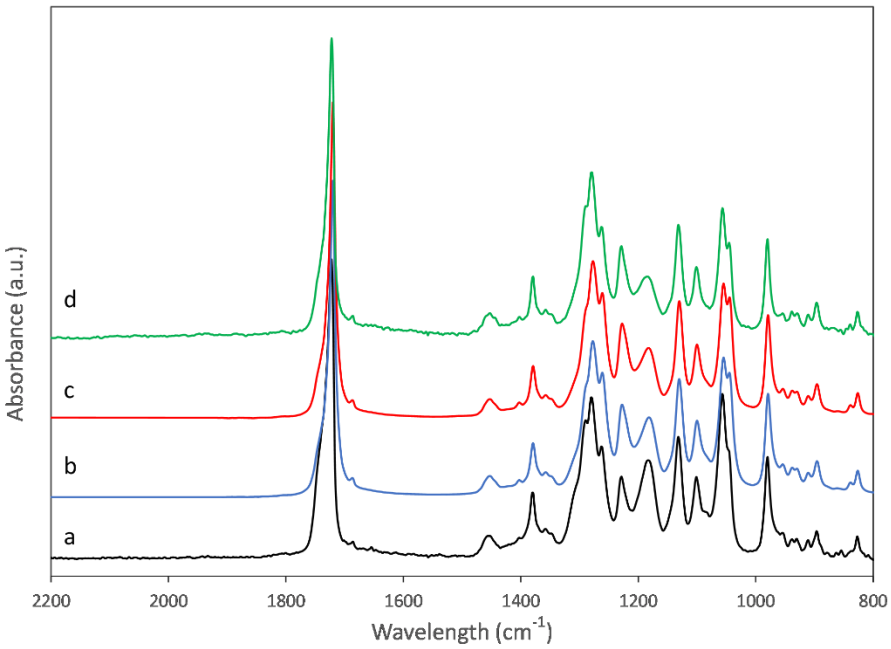

Figure 2. FTIR spectra of PHB electrospun fibers UV-irradiated for (a) 0 h, (b) 50 h, (c) 250 h, and (d) 500 h.

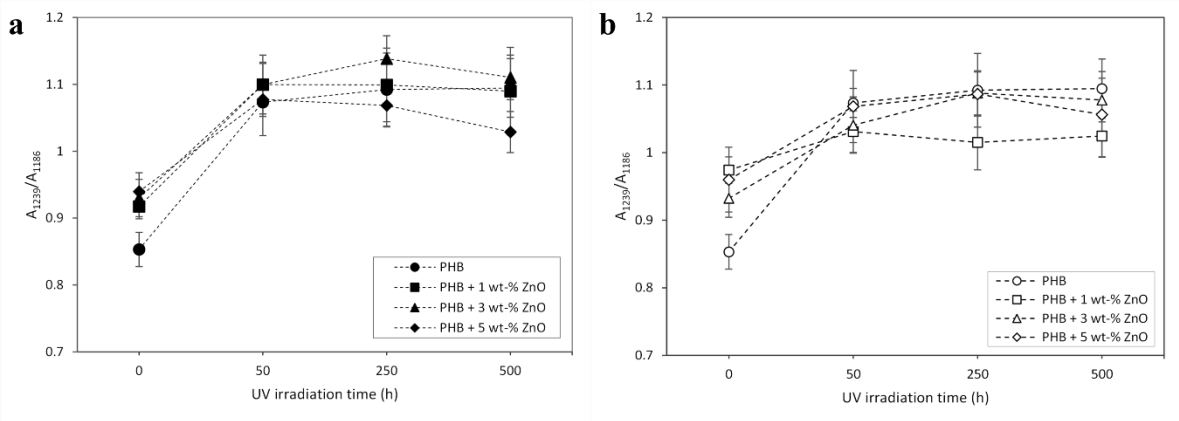

Figure 3. A_{1230}/A_{1186} ratio as a function of UV irradiation time and ZnO concentration for PHB mats derived from (a) electrospinning and (b) electrospinning/electrospraying techniques, the bars represent the standard deviation (n = 2-3 experiments) which was between 3 and 8%.

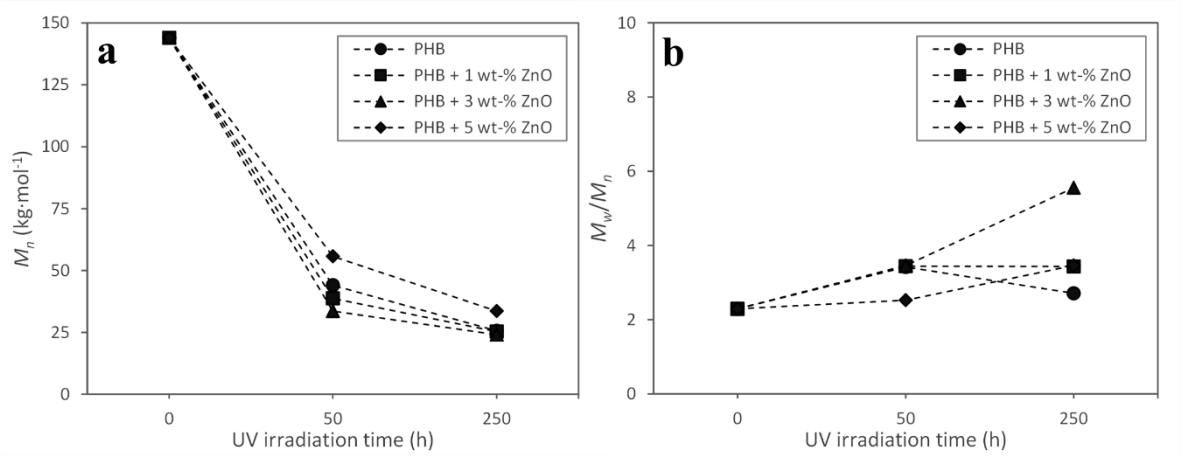

Figure 4. (a) Number-average molar mass (M_n) and (b) dispersity index (M_w/M_n) for the electrospun PHB/ZnO materials as a function of UV irradiation time and ZnO concentration.

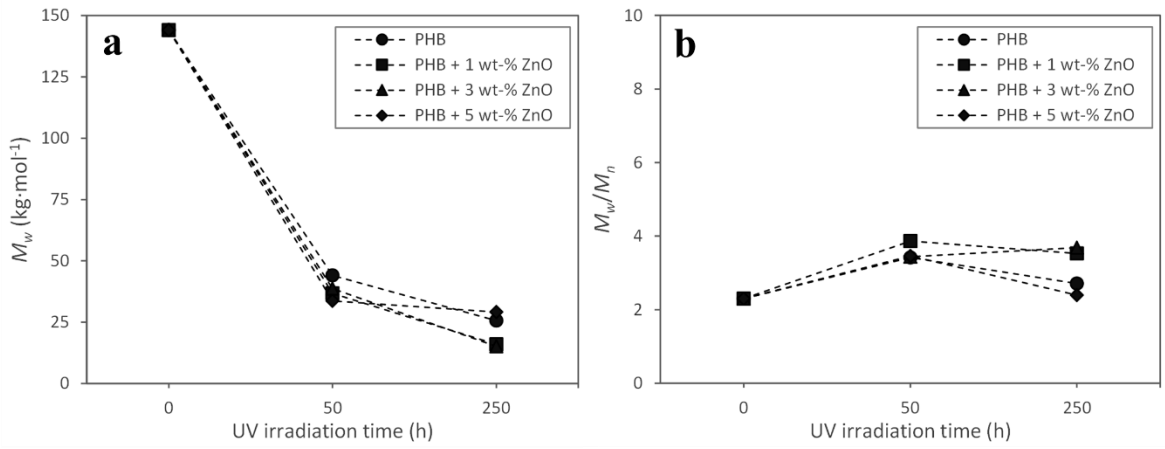

Figure 5. (a) Number-average molar mass (M_n) and (b) dispersity index (M_w/M_n) for the electrospun/electrosprayed PHB/ZnO materials as a function of UV irradiation time and ZnO concentration.

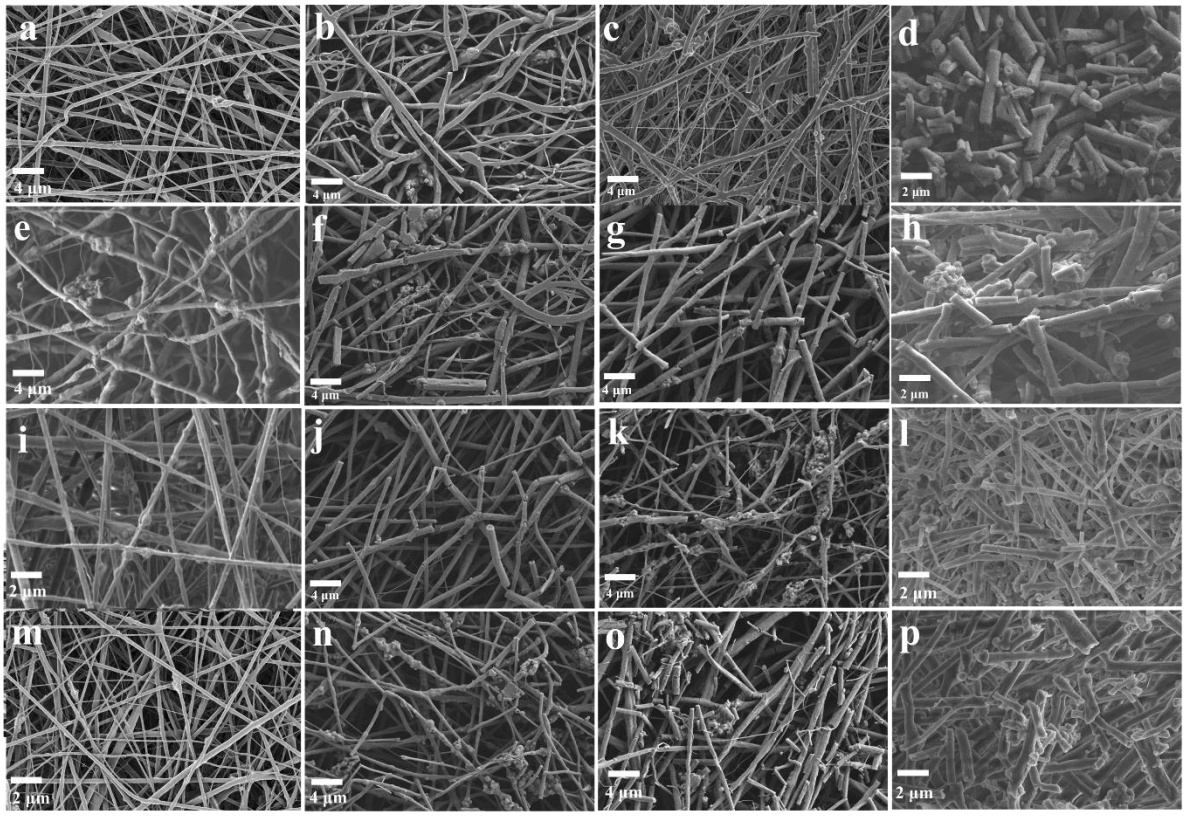

Figure 6. SEM micrographs of the electrospun PHB/ZnO materials containing (a-d) 0, (e-h) 1, (i-l) 3 and (m-p) 5 wt-% ZnO, and subjected to (a, e, i, m) 0 h, (b, f, j, n) 50 h, (c, g, k, o) 250 h, and (d, h, l, p) 500 h of UV irradiation.

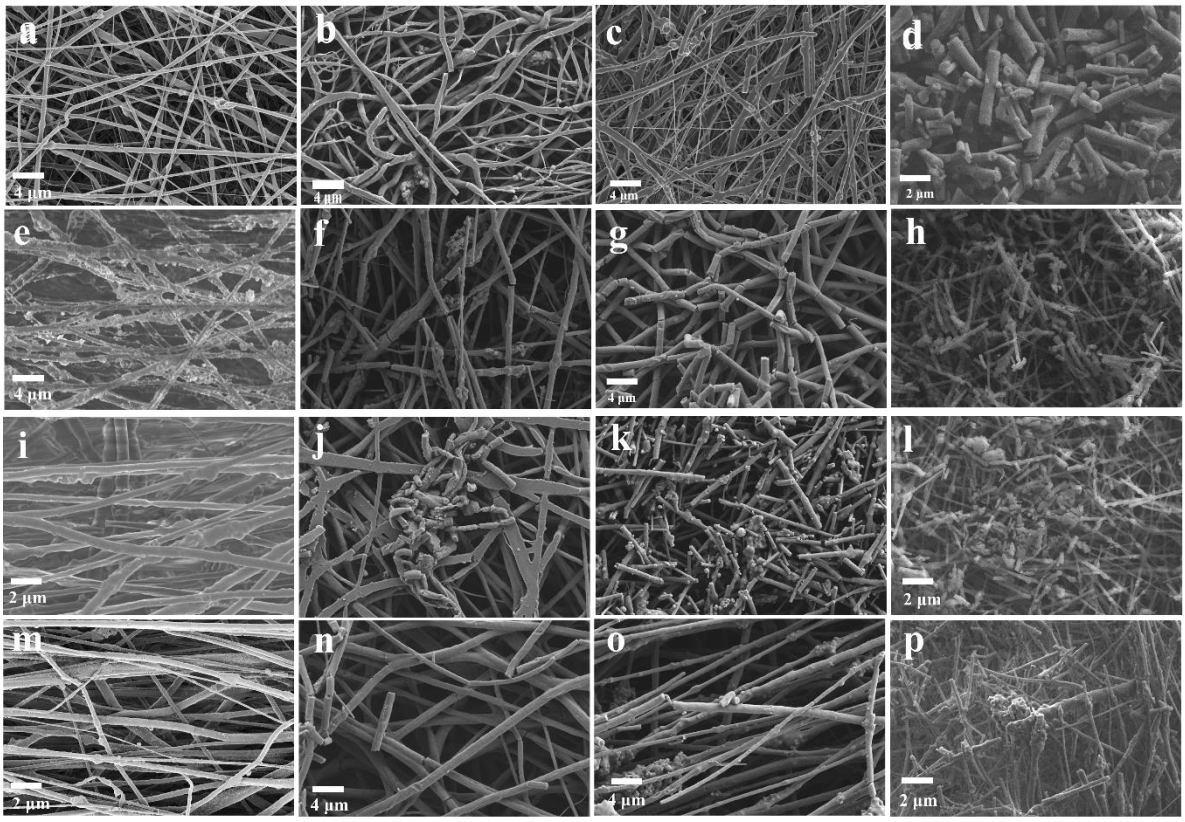

Figure 7. SEM micrographs of the electrospun/electrosprayed PHB/ZnO materials containing (a-d) 0, (e-h) 1, (i-l) 3 and (m-p) 5 wt-% ZnO, and subjected to (a, e, i, m) 0 h, (b, f, j, n) 50 h, (c, g, k, o) 250 h, and (d, h, l, p) 500 h of UV irradiation.